THE JOURNAL OF COMPARATIVE NEUROLOGY 459:77–89 (2003)

Ultrastructural Examination of the Somatic Innervation of Ventrotubercular Cells in the Rat

DAVID R. FRIEDLAND,[1] TAN PONGSTAPORN,[1] JOHN R. DOUCET,[1] AND DAVID K. RYUGO[1,2]*

[1]Department of Otolaryngology–Head and Neck Surgery, Center for Hearing Sciences, Johns Hopkins University School of Medicine, Baltimore, Maryland 21205

[2]Department of Neuroscience, Center for Hearing Sciences, Johns Hopkins University School of Medicine, Baltimore, Maryland 21205

ABSTRACT

Ventrotubercular cells are multipolar cells in the ventral cochlear nucleus (VCN) that project a collateral axon to the ipsilateral dorsal cochlear nucleus (DCN). These cells are thought to be involved in sensitizing DCN output neurons to spectral shapes that represent the location of a sound source in space. The present report focused on the neuronal composition of this pathway. Intracellular labeling studies in cats and mice have described two types of ventrotubercular cells (Smith and Rhode [1989] J Comp Neurol. 282:595–626; Oertel et al. [1990] J Comp Neurol. 295:136–154). In cats, one difference between the two classes is that type I multipolar neurons have fewer than 35% of their somata apposed by terminals, whereas type II cells have greater than 70% apposition values. Intracellular recordings from single cells, however, are difficult and thus limit the yield of data. We investigated whether a two-component description of the ventrotubercular pathway was representative of a larger population. This issue was addressed by retrogradely labeling ventrotubercular neurons with an extracellular injection of biotinylated dextran amine into the DCN of rats. These injections labeled many VCN neurons, thus providing a more complete view of the pathway than previous studies. Thirty-eight labeled cells were selected for electron microscopic analysis with respect to their location, cell body size, and ultrastructural morphology. We observed labeled type I and type II neurons, but unlike ventrotubercular cells in cats, many of these neurons in rats (17 of 38 cells) had appositions between 35% and 70%. On the basis of this analysis, a third class of ventrotubercular cell, called the *adendritic neuron*, was revealed. Adendritic neurons have small somata with many filopodial appendages, no observable dendrites, and high percentage of terminal appositions (>80%). The results demonstrated that the ventrotubercular pathway in the rat is diverse. J. Comp. Neurol. 459:77–89, 2003. © 2003 Wiley-Liss, Inc.

Indexing terms: auditory system; electron microscopy; hearing; multipolar cells

Neurons of the ventral cochlear nucleus (VCN) have been described and grouped according to many morphologic features (Osen, 1969; Brawer et al., 1974; Adams, 1979, 1983; Cant, 1981, 1982; Warr, 1982; Ryugo and Willard, 1985; Hackney et al., 1990) and physiologic response properties (Pfeiffer, 1966; Evans and Nelson, 1973; Young and Brownell, 1976; Young et al., 1988; Blackburn and Sachs, 1989; Rhode and Greenberg, 1992). An important goal remains, to determine what structural features underlie the distinct response properties to sound. In this context, we examined the ultrastructural morphology of VCN neurons that project their axons to the ipsilateral dorsal cochlear nucleus (DCN).

The axonal pathway produced by VCN neurons projecting to the DCN has been referred to as the *ventrotubercular tract* (Lorente de Nó, 1981). This projection has two

Portions of this work were presented in preliminary form at the 25th Annual Meeting of the Association for Research in Otolaryngology, 2002.

Grant sponsor: National Institute of Health/National Institute on Deafness and Other Communication Disorders; Grant numbers: DC00232, DC00023, and DC04505; Grant sponsor: Herbert Silverstein grant; Grant sponsor: American Academy of Otolaryngology Foundation.

*Correspondence to: David K. Ryugo, Center for Hearing Sciences, Traylor 510, Johns Hopkins University School of Medicine, 720 Rutland Avenue, Baltimore, MD, 21205. E-mail: dryugo@bme.jhu.edu

Received 28 August 2002; Revised 29 October 2002; Accepted 12 December 2002

DOI 10.1002/cne.10603

Published online the week of March 3, 2003 in Wiley InterScience (www.interscience.wiley.com).

© 2003 WILEY-LISS, INC.

components. There is a microneuronal pathway initiated by small cells in the granule cell domain and a magnocellular projection from cells in the core of the VCN (Adams, 1983; Snyder and Leake, 1988; Doucet and Ryugo, 1997; Ostapoff et al. 1999). In this report, the term *ventrotubercular* refers to the large cells in the VCN core that have a projection to the DCN. Ventrotubercular neurons belong to a morphologic class of VCN neurons termed *multipolar* (or stellate) cells. In cats, an intracellular recording and staining study demonstrated at least two different types of ventrotubercular cells (Smith and Rhode, 1989). One type corresponded to the physiologic units named *sustained choppers* (ChS). Light microscopic (LM) observations showed that this class had dendrites that were confined to a VCN isofrequency sheet and an axon that exited the cochlear nucleus via the trapezoid body (a collateral axon projected to the DCN). With the electron microscope (EM), these cells were observed to be type I neurons that have few inputs directly on the soma (Cant, 1981). Most VCN multipolar neurons that project to the contralateral inferior colliculus (IC) are type I and they appear to be excitatory (Cant, 1982; Alibardi, 1998a; Oliver, 1987). The second class of ventrotubercular cell was composed of onset chopper (OnC) units. The dendrites of OnC units were oriented perpendicular to VCN isofrequency sheets, and their axon exited the cochlear nucleus via the dorsal or intermediate acoustic stria. These cells were called *type II neurons* and receive many inputs on the soma (Cant, 1981). VCN neurons that project to the contralateral cochlear nucleus have LM morphology similar to that of OnC cells (Cant and Gaston, 1982; Schofield and Cant, 1996), exhibit features of type II cells (Alibardi, 1998b), and many immunostain for glycine (Wenthold, 1987; Alibardi, 1998b). In mice, ventrotubercular neurons that were filled intracellularly by using an in vitro brain slice preparation also comprised two types (Oertel et al., 1990). T-stellate cells in mice have LM features similar to those of type I/ChS cells in cats, and D-stellate cells in mice resemble type II/OnC neurons in cats. Collectively, these studies suggested that the ventrotubercular pathway is composed of two distinct components.

Intracellular recording and staining of single neurons provide direct comparisons between structural features and physiologic properties. The difficulty of this technique, however, limits the yield and scope of such comparisons. In contrast, studies that have examined large populations of cochlear nucleus neurons with the use of extracellular recording and staining techniques tend to reveal more neuronal types and suggest greater variability (e.g., Bourk, 1976; Snyder and Leake, 1988; Blackburn and Sachs, 1989, 1992; Palmer et al., 1996; Doucet and Ryugo, 1997; Ostapoff et al., 1999; Alibardi, 2001). The results of such studies, however, are typically more difficult to interpret. Both approaches are useful, but reconciling their differences is necessary for modeling and understanding the influence of the ventrotubercular pathway on signal processing in the DCN.

We addressed this issue by examining the ultrastructural morphology of ventrotubercular cells in rats, concentrating primarily on the percentage of the cell body apposed by synapses (percent apposition). This approach was taken for two reasons. First, intracellular studies of these neurons predicted that we should observe two distinct populations of cells. There would be those with few synapses on the cell body (type I) and those with many (type II; Smith and Rhode, 1989). Measuring percent apposition would directly address the two-component hypothesis for the ventrotubercular pathway. Second, modeling studies suggested that the number and types of inputs on the cell body are important features in determining how a cell responds to sound (Banks and Sachs, 1991; Hewitt and Meddis, 1993; Wang and Sachs, 1995). We postulated that physiologic variability in the ventrotubercular pathway might be revealed by measuring percent apposition. Ventrotubercular cells were labeled by making an extracellular injection of biotinylated dextran amine (BDA) into a restricted frequency region of the DCN. We examined the size of the cell bodies, the topography of their projections to the DCN, and the amount of somatic input. We found that the ventrotubercular pathway in rats is more diverse than what has been reported for other species.

MATERIALS AND METHODS

Surgical preparation

This report is based on data from seven adult male Sprague-Dawley rats weighing between 250 and 400 g. All experiments were performed in accordance with National Institutes of Health guidelines and the approval of the Animal Care and Use Committee of the Johns Hopkins University Medical School. Rats were anesthetized with an injection of sodium pentobarbital (40 mg/kg, intraperitoneally) followed by an injection of atropine sulfate to reduce secretions (0.1 ml, intramuscularly). Depth of anesthesia was determined by paw pinch reflex, and surgery was begun only after areflexia was achieved. A sagittal incision was made through the soft tissue overlying the dorsal cranium, and the skin and muscle were reflected laterally. The occipital bone on one side was removed to expose the hemicerebellum, which was aspirated from vermis to flocculus to expose the DCN. A glass electrode (tip inner diameter: 10–20 μm) was filled with a 10% (w/v) solution of BDA (molecular weight 10,000; Molecular Probes, Eugene, OR) in 0.01 M phosphate buffer (pH 7.4). The electrode was advanced with a micromanipulator into the DCN to a depth of 200 to 250 μm below the surface. Iontophoretic injection of the BDA was achieved with positive current pulses (5 μA, 7 seconds on and 7 seconds off, 3–5 minutes). Subsequently, the wound was closed with surgical clips, and the rat was allowed to recover under a warming lamp with free access to food and water in the postoperative period.

Tissue processing

Approximately 24 hours after injection of BDA, the rat was administered a lethal intraperitoneal dose of sodium pentobarbital. When the animal was areflexic to a paw pinch, it was transcardially perfused with 10 ml of 0.1 M cacodylate buffer (pH 7.3) with 1% sodium nitrate at 37°C and then 250 ml of 0.1 M cacodylate buffer (pH 7.3) containing 2% paraformaldehyde and 2% glutaraldehyde at 4°C. The brain was dissected from the skull and postfixed in the same fixative for 1 hour at room temperature. The tissue was then trimmed around the cochlear nuclei and embedded in gelatin albumin. Vibratome sections were cut at 60 μm in the coronal plane, collected in 0.1 M cacodylate buffer (pH 7.3), and processed in serial order. Sections were incubated overnight in avidin-biotin com-

plex (ABC Elite, Vector Laboratories, Burlington, CA) at 4°C on a shaker table. The following day, the sections were washed twice in 0.05 M cacodylate buffer (pH 7.3) for 5 minutes each and then incubated in a solution containing 0.0125% 3,3′-diaminobenzidine (DAB), 0.25% nickel ammonium sulfate and 0.35% imidazole in 0.05 M cacodylate buffer for 10 minutes. Fresh nickel/DAB with the addition of hydrogen peroxide (v/v, 0.02%) was added to the sections and allowed to incubate in the dark for 15 minutes. Sections were washed twice in 0.05 M cacodylate buffer and examined with an inverted microscope for labeling of ventrotubercular cells. Sections that contained few or no labeled cells were mounted on subbed slides, air dried overnight, counterstained lightly with cresyl violet, and coverslipped with Permount.

Electron microscopy

Sections that contained labeled ventrotubercular cells were processed for EM. They were placed in 1% OsO_4 for 15 minutes, rinsed five times in 0.1 M maleate buffer (pH 5.0) for 5 minutes each, and stained in 1% uranyl acetate in methanol overnight. The following day, sections were washed in 0.1 M maleate buffer, dehydrated in a graded series of increasing ethanol concentration, infiltrated with Epon, and embedded between sheets of Aclar. Sections were hardened overnight at 70°C and taped to microscope slides for LM examination.

Relevant sections were photographed under 2.5× and 10× objectives with a chilled CCD color camera attached to a Macintosh computer. The region of the VCN containing labeled cells was cut from the Aclar and re-embedded in Epon in BEEM capsules. Capsules were hardened at 70°C, and block faces were trimmed for ultrathin sectioning. The position of cells relative to blood vessels, tissue borders, and neighboring cells was mapped with a LM (100× objective). A semithin section (250 nm) was cut and stained with toluidine blue. Labeled cells could be identified in the semithin sections by their gray-blue cytoplasm. Serial ultrathin sections (75 nm) were taken through each labeled cell in the block. Sections were collected on grids coated with Formvar, counterstained with 7% uranyl acetate, and maintained in serial order. Ultrathin sections were viewed and photographed with a JEOL 100CX EM.

Data analysis

Cell location within the VCN. Labeled neurons were sampled from a region of the VCN spanning the posterior VCN to the region immediately anterior to the auditory nerve root. Injections of BDA into the DCN labeled only a few neurons in the anteroventral cochlear nucleus (Doucet and Ryugo, 1997). LM images of labeled cells were captured (10× objective) and imported into Adobe Photoshop 6.0. We measured the distance of each labeled cell from the medial border of the VCN and normalized this value by dividing it by the width of the VCN in the medial/lateral plane. A value near zero would signify that the cell was near the medial edge of the VCN, whereas a value of one would indicate it was near the lateral edge.

Cell size and synaptic appositions. For each cell, we chose two sections through the nucleus (and the nucleolus, if present) that were separated by at least 1.5 μm. In each section, the cell was photographed at 2,700× for the analysis of somatic morphology on an EM. Photomontages were constructed of the cell perimeter at 14,000× for the analysis of synaptic appositions and measurement of contact area. For four neurons, these measurements were made for serial sections through the entire cell. We determined that analysis of two sections through the nucleus provided similar results as analysis of serial sections for both somatic area and synaptic appositions. Therefore, we restricted our analysis to two sections for the remaining labeled cells of the study. Negatives were digitized by high resolution scanning on a Leafscan45 attached to a Macintosh computer.

The outline of the somatic plasma membrane was drawn from micrographs (2,700× magnification). The density of ribosomes was used to separate cell body from dendrite. Because the region around the base of the primary dendrite tended to be covered with endings, we considered the cut edge between soma and dendrite to be apposed by an ending. The perimeter and area were then calculated by using image processing software (Image Processing ToolKit 3.0 plug-in for Photoshop, Reindeer Games, Asheville, NC). The total length of terminal apposition was calculated (14,000× magnification) and then divided by the cell perimeter to determine the percentage of the surface contacted by synaptic endings. This procedure was performed for each of the two sections through each cell and the mean was calculated. Means and standard deviations are provided where appropriate. Regression analysis determined variables that correlated with percent apposition. Analysis of variance was used to compare quantitative measures of cell size, terminal morphology, and synaptic apposition between cell populations.

RESULTS

Light microscopy

Retrograde labeling in the VCN. As we described previously (Doucet and Ryugo, 1997), a small injection of BDA into the DCN (Fig. 1A) produces a distinctive pattern of labeling in the VCN (Fig. 1B). Nearly every coronal section through the cochlear nucleus contained a labeled band filled with axons, terminals, dendrites, and cell bodies. The dorsal/ventral position of the band was topographically related to the medial/lateral location of the injection site in the DCN. The topographic relationship corresponded to the known tonotopic maps of the nucleus (Rose et al., 1959; Bourk et al., 1981; Spirou et al., 1993) and the inputs from auditory nerve fibers (Ryugo and May, 1993). We refer to this labeled band of cells and fibers as the *isofrequency band*.

We previously used LM criteria (e.g., soma size, dendritic morphology, and orientation) to identify three different classes of ventrotubercular cells in rats: planar, radiate, and marginal (Doucet and Ryugo, 1997). Planar cells have medium-size cell bodies and dendrites oriented parallel to the plane of VCN isofrequency sheets. Their somata are located primarily within the isofrequency band; that is, they project tonotopically to the DCN. These and other morphologic features suggested that planar cells correspond to T-stellate cells in mice and type I/ChS cells in cats (see Discussion in Doucet et al., 1999). Radiate cells have large cell bodies and dendrites oriented perpendicular to the plane of VCN isofrequency sheets (Fig. 1B). Their somata are found within and outside the isofrequency band. Radiate cells seem to correspond to D-stellate cells in mice and type II/OnC cells in cats. Marginal cells are small neurons in a region of the VCN

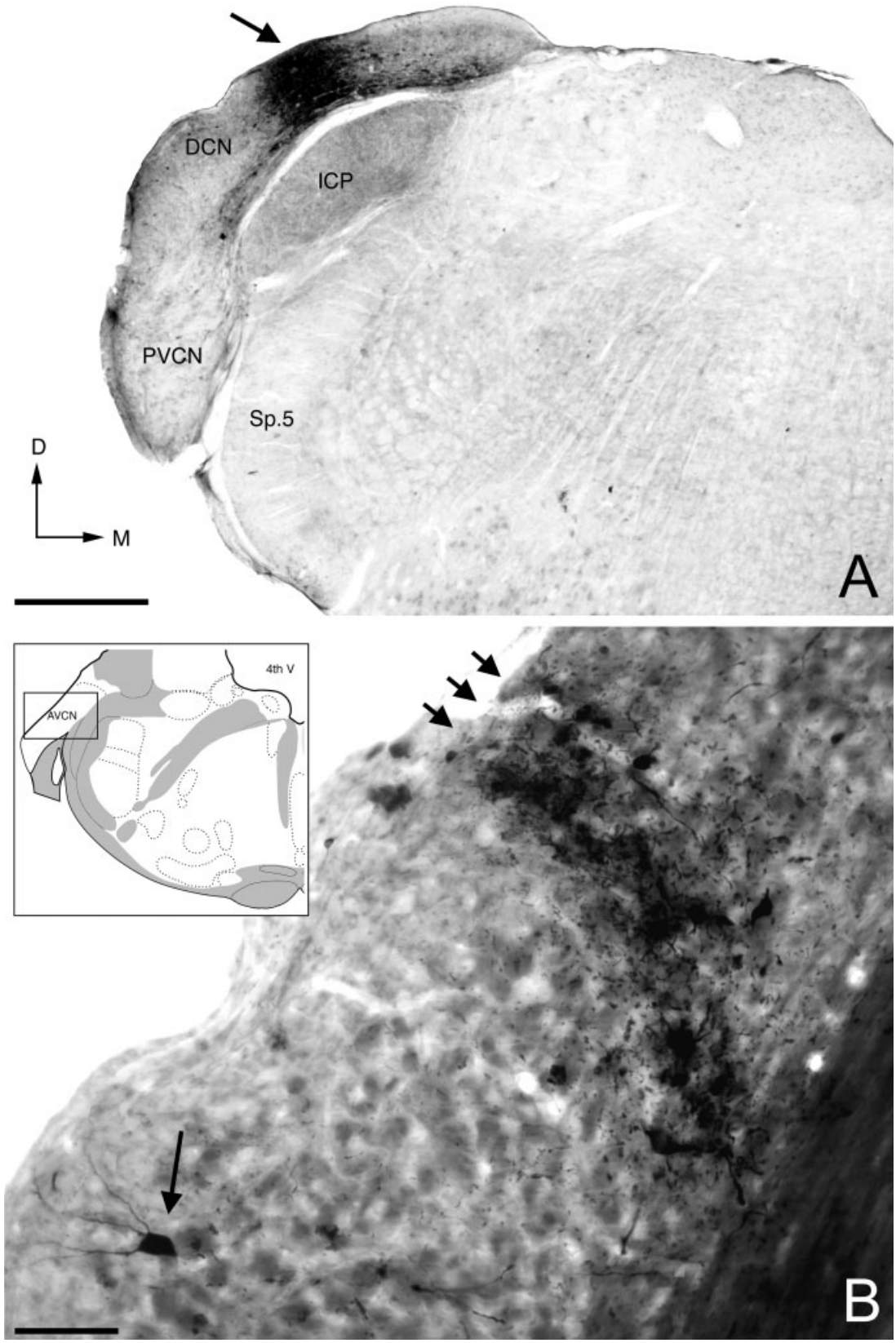

Fig. 1. An injection of biotinylated dextran amine into the dorsal cochlear nucleus (DCN) retrogradely labels a sheet of axons, terminals, and neurons in the ventral cochlear nucleus (VCN). **A:** Photomicrograph of the injection site in the DCN (arrow), viewed in the coronal plane. The injection site is restricted to the DCN. The absence of labeled DCN pyramidal cells lateral to the injection and labeled octopus cells in the VCN is evidence that there was no spread into the output tracts. **B:** Photomicrograph of a section through the VCN in the same case (inset drawing illustrates brainstem location). The stripe of labeled elements in the VCN defines the isofrequency band (three short arrows) and is characterized primarily by labeled neurons whose dendrites lie within the band. The large cell outside the stripe is a radiate cell (large arrow) and exhibits dendritic projections that cross isofrequency sheets. 4th V, fourth ventricle; AVCN, anteroventral cochlear nucleus; D, dorsal; DCN, dorsal cochlear nucleus; ICP, inferior cerebellar peduncle; M, medial; Sp.5, spinal track of the trigeminal nerve; PVCN, posteroventral cochlear nucleus. Scale bars = 500 μm in A, 100 μm in B.

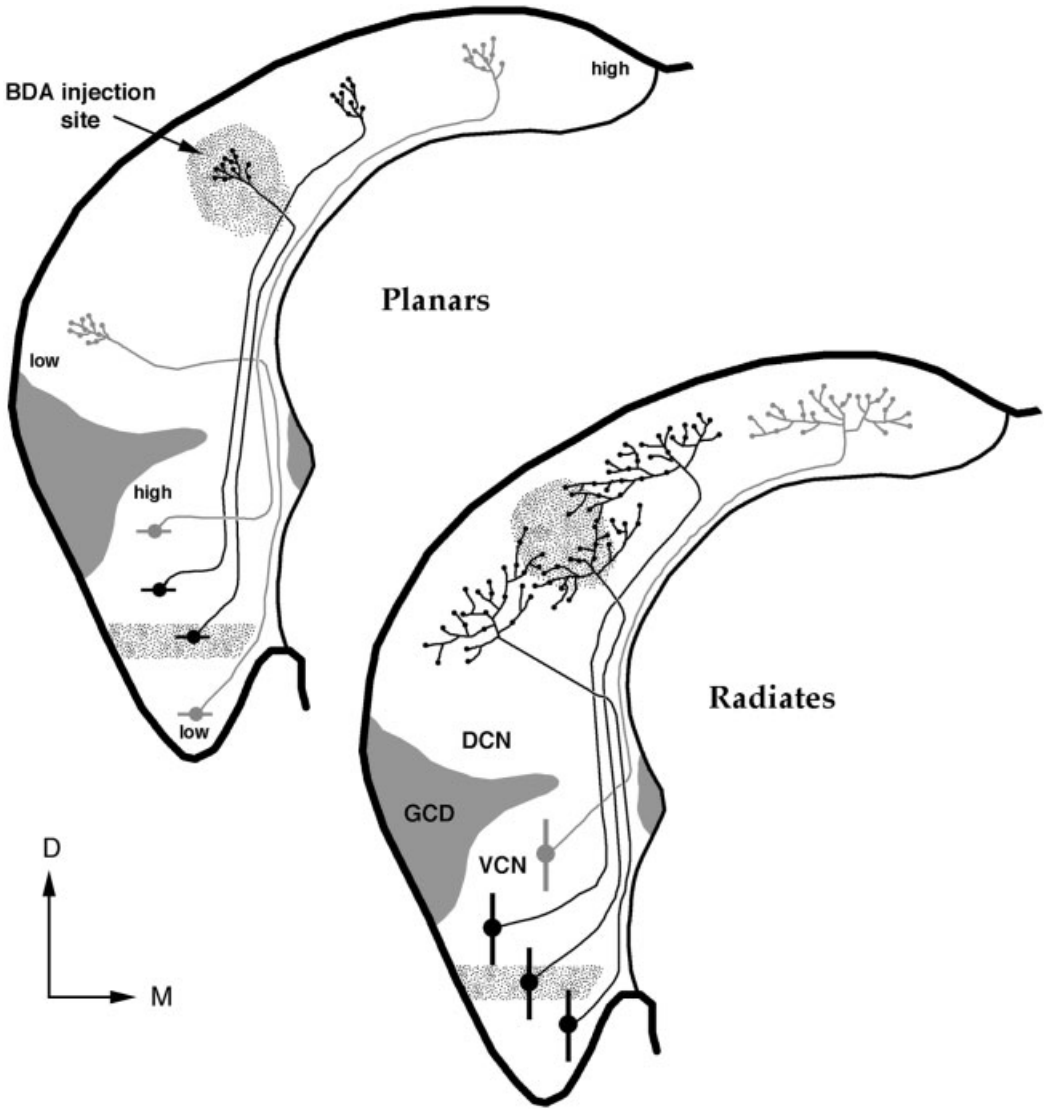

Fig. 2. Schematic representation of the labeling patterns in the ventral cochlear nucleus (VCN) after an injection (indicated by circular stippled region) into the dorsal cochlear nucleus (DCN). The hypothetical distribution of planar and radiate cells is based on our previous work (Doucet and Ryugo, 1997). Planar cells are hypothesized to have narrow terminal fields in the DCN, and most labeled cell bodies would be found in the isofrequency band (indicated by stippled stripe in the VCN). The isofrequency band is in a frequency region corresponding to the DCN injection site. A few planar cells might be found dorsal to the isofrequency band as their axons pass through the injection site en route to their termination in higher frequency regions. Radiate cells are hypothesized to have broad terminal axonal fields in the DCN, so their cell bodies would tend to be distributed above and below the labeled VCN stripe. D, dorsal; GCD, granule cell domain; M, medial.

between the shell of granule cells surrounding the nucleus and the magnocellular core. This article focuses on the ultrastructural morphology of planar and radiate cells in the magnocellular core.

Our LM observations suggested that the ventrotubercular pathway in rats (like mice and cats) is composed of at least two components: planar and radiate. The objective was to determine whether ultrastructural features of planar and radiate neurons are consistent with this two-component description. Our working hypothesis was that planar cells correspond to type I cells (few inputs on the soma), whereas radiate cells correspond to type II cells (many inputs on the soma). We could not test this hypothesis directly with EM because too many cells and dendrites are filled in the VCN after a DCN injection. The number of filled structures prevented reconstructing and assigning all labeled cells into the planar or radiate class. However, if this hypothesis is true, we can predict the distribution of type I and type II cells in the VCN for a small injection of BDA into the DCN. These two hypothetical distributions are schematized for an injection in the mid-DCN (Fig. 2). BDA-filled cells are shown in black. The isofrequency band (stippled region in VCN) should be filled with planar (type I) cells. Retrogradely labeled planar cells also might be found dorsal to the isofrequency band. Such planar cells would be labeled if their axons

traversed the injection site en route to more medial (high frequency) regions of the DCN (Fig. 2). Radiate cells (type II) should be found within and outside the isofrequency band. These proposed distributions of type I and type II cells are tested below.

Electron microscopy

The ultrastructural features of 38 cells filled with BDA were examined with the EM. Twenty-four neurons were located within the isofrequency band, and 14 were outside (five were ventral to the band). Although retrogradely labeled cells outside the isofrequency band comprised approximately 20% of all labeled cells after a small injection into the DCN, the biased distribution of analyzed cells in this report is a deliberate result of our sample selection.

The location of each cell was normalized along the medial/lateral extent of the VCN. This analysis examined whether synaptic input to the cell body was related to the medial/lateral position in the nucleus. For the 24 cells within the isofrequency band, the range in the medial/lateral ratio was from 0.24 to 0.83, with a mean of 0.51 ± 0.19 (where zero was medial and one was lateral). The analyzed cells were evenly distributed within the isofrequency band (Fig. 9). For the cells chosen outside the isofrequency band, the range was from 0.16 to 0.76, with a mean of 0.41 ± 0.22. These results demonstrated that our chosen population of neurons is restricted to the core of the VCN (i.e., planar and radiates). Our ultrastructural analyses showed no morphologic features that correlated with the medial/lateral position of the labeled neurons.

Axosomatic terminal apposition for planar and radiate cells. Labeled ventrotubercular cells, when examined with EM, showed a relatively wide variation in axosomatic contacts. If labeled cells found within the isofrequency band are planar cells and those outside the band are radiate cells, then a corollary is that planar cells would have few axosomatic contacts and radiate cells would have many. A histogram of percent apposition for the 38 ventrotubercular cells (Fig. 3) illustrates that some ventrotubercular neurons had few somatic terminals (<35%, n = 10), whereas others had many (>70%, n = 11). Nearly 45% (17 of 38) of the neurons, however, had percent appositions between these two values. This latter observation was surprising for two reasons. First, none of the intracellularly labeled ventrotubercular cells in cats had percent appositions between 38% and 70% (Smith and Rhode, 1989). Second, a random sample of percent appositions for multipolar/stellate cells in cats found that only 9% (2 of 23) had percent appositions between 38% and 70% (Cant, 1981). Given the correspondence between the LM features of ventrotubercular cells in cats and rats, we did not expect this apparent lack of correspondence between their ultrastructural features.

Distribution and size of cell types. Perhaps ventrotubercular cells in cats and rats are only slightly different. In other words, planar (type I) cells may have relatively few synapses on the soma and radiate (type II) cells may have many, but the distributions of percent apposition may overlap in rats. This proposal can be evaluated by comparing the percent apposition of the neurons with their location in the VCN. All analyzed cells were divided into three groups on the basis of the position of their somata with respect to the isofrequency band (Fig. 4): dorsal to the band (nine cells in Fig. 4A), inside the band (24 cells in Fig. 4B), and ventral to the band (five cells in Fig. 4C). The data are presented in this manner to facilitate comparisons with the hypothetical distribution of planar and radiate cells (Fig. 2). In each panel, the somatic area of the cells is plotted against its percent apposition. A horizontal line is positioned at 250 μm^2 because cells having somata less than this value are likely planar cells (Doucet et al., 1999). Percent appositions less than 50% are be referred to as *low*, whereas those above 50% are referred to as *high*.

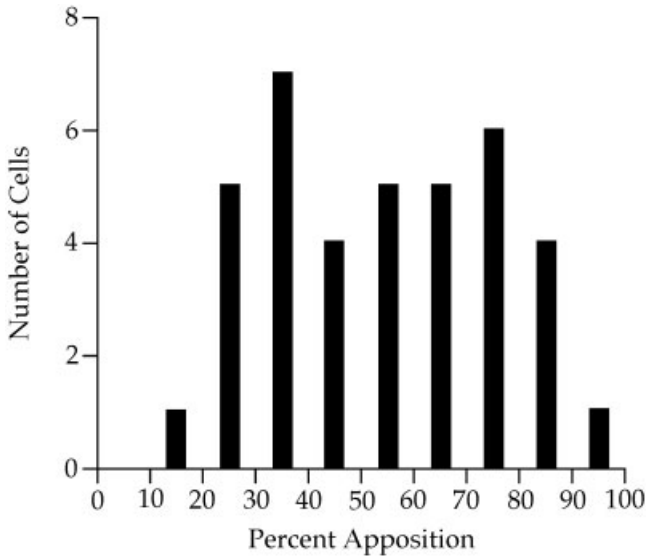

Fig. 3. Histogram of percent appositions for 38 ventrotubercular cells. The histogram is not clearly bimodal as observed for stellate cells in cats (Cant, 1981), but there is a suggestion of two peaks. Neurons having percent appositions lower and higher than 50% are referred to as *low* and *high* percent apposition cells, respectively.

Several features of the distribution and size of ventrotubercular cells correlated with the amount of synaptic input they received on their somata. Outside the isofrequency band (Fig. 4A,C), most cells had high percent appositions. In fact, cells that had high percent appositions were observed in all three regions (Fig. 4A–C). In contrast, cells that had low percent appositions were found within (Fig. 4B) and dorsal (Fig. 4A) to the band. Within the isofrequency band (Fig. 4B), a mixture of cell types was encountered. Five cells in the isofrequency band had small somata, very high percent appositions (>80%), and additional features (see below) that clearly distinguished them from other ventrotubercular neurons (plus signs in Fig. 4B). These cells are referred to as *adendritic neurons*. It is important to note that adendritic neurons appear to be different from marginal cells. Marginal cells are a class of small ventrotubercular cell that is located between the granule cell domain and the magnocellular core of the VCN (Doucet and Ryugo, 1997). In contrast, adendritic neurons were intermingled with planar and radiate cells in the VCN core (Fig. 9). If they are treated as a third group, then the average somatic area of cells that had high percent apposition (316.9 ± 131 μm^2) was significantly larger than those having low percent apposition (208.3 ± 74 μm^2; $P < 0.005$) and adendritic neurons (149.4 ± 31 μm^2; $P < 0.001$).

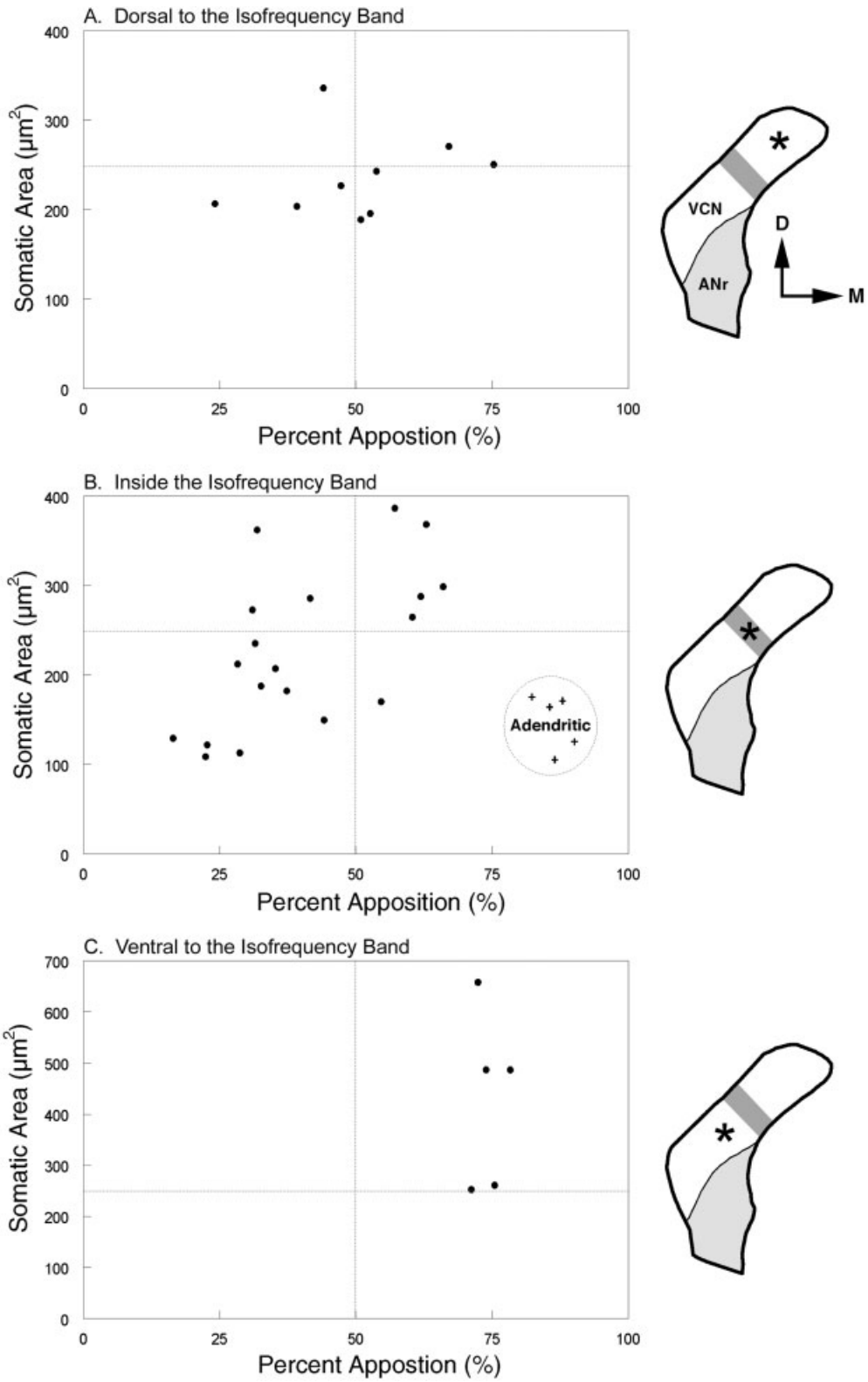

Fig. 4. Distribution of projections for low and high percent apposition cells to the dorsal cochlear nucleus. We measured the somatic area of the neuron and the percent apposition for 38 cells. These two measurements are displayed as scatter plots where each filled circle represents one cell. The schematic to the right of each plot displays the position of the cells (asterisk) with respect to the isofrequency band (gray region). **A:** Data are displayed from cells dorsal (D) to the isofrequency band. **B:** These data were obtained from cells within the isofrequency band. **C:** These data were obtained ventral to the band. The vertical line at 50% divides the cells into two groups that have low or high percent apposition. The horizontal line roughly divides the cells into planar neurons (below the line) and radiate neurons (above the line). These plots are discussed in the text in the context of examining the hypothesis that planar cells have low percent apposition, whereas radiate neurons have high percent apposition. ANr, auditory nerve root; M, medial; VCN, ventral cochlear nucleus.

Ultrastructural morphology. Ultrastructural descriptions of stellate (multipolar) cells attempted to define features such as cell body shape, stacking of the endoplasmic reticulum, distribution of mitochondria, packing of ribosomes, and presence or absence of somatic spines that correlated with the degree of synaptic input on the cell body (Cant, 1981; Smith and Rhode, 1989). For the labeled ventrotubercular cells in this study, the shapes of most somata were ovoid or fusiform. The mitochondria appeared to be randomly distributed throughout the cytoplasm. No particular pattern was observed with respect to the distribution of the Golgi apparatus or endoplasmic reticulum. Nuclear shape was another diverse feature, with most being round and smooth, but approximately 20% had indentations or deep invaginations. Most nuclear profiles contained one large nucleolus surrounded by euchromatin, with no areas of heterochromatin, reflecting high metabolic and transcriptional activities in these neurons. In short, we could not identify intracellular characteristics that distinguished one ventrotubercular cell type from another.

Labeled ventrotubercular cells that were distributed within the labeled band and exhibited no somatic filopodia tended to have low somatic apposition values (Figs. 4, 5). Large, labeled, ventrotubercular cells, regardless of their location, tended to have high somatic apposition values (Fig. 6). The morphology of adendritic cells was markedly different from that of other ventrotubercular cells (Fig. 7). For example, no dendrites were observed for adendritic cells, and they were studded with short, finger-like projections arising from the soma and extending into the surrounding neuropil (Fig. 8). These filopodial projections insinuated themselves between the numerous synaptic terminals that apposed the somatic surface. In some respects, adendritic neurons resembled chestnut cells that were previously described in the granule cell domain (Weedman et al., 1996), and we argue that they represent a separate cell grouping.

DISCUSSION

We examined the ultrastructural morphology of ventrotubercular neurons in the rat that were retrogradely labeled with an extracellular injection of BDA into the DCN. With the LM, we confirmed our previous reports that this pathway is composed of at least two types of neurons in the VCN core: planar and radiate cells. EM analysis of these cells revealed two new findings. First, the somatic coverage by synaptic endings demonstrated differences when comparing stellate cells of rats and cats. Percent appositions for cat multipolar cells fell into two distinct groups, whereas those in rats formed a continuum from low to high. Second, a new type of ventrotubercular cell, called the adendritic neuron, was suggested by using the EM. Adendritic neurons have small somata, no observable dendrites but many somatic filopodia, a high percent apposition (>80%), and a tonotopic projection to the DCN. With respect to the overall composition of the ventrotubercular pathway, it is important to note that this study did not analyze the marginal cells that project to the DCN (Doucet and Ryugo, 1997). Collectively, these observations led to the general conclusion that the ventrotubercular pathway, at least in the rat, is diverse.

Composition of ventrotubercular pathway: LM versus EM observations

One goal of this study was to correlate ultrastructural characteristics of ventrotubercular cells with previous descriptions of their LM morphology. Our working hypothesis was that planar and radiate cells in the rat (LM definition, Doucet and Ryugo, 1997) corresponded to type I and type II stellate neurons in the cat (EM definition, Cant, 1981). Testing this hypothesis was rendered moot after observing the distribution of synaptic profiles for ventrotubercular cells in the rat (Fig. 3). Nearly half of these cells fell outside the classic definitions for type I and type II cells.

Nevertheless, we made several observations relevant to the proposed correspondence between planar/type I cells and radiate/type II cells. Planar cell bodies are significantly smaller than those of radiate cells (Doucet and Ryugo, 1997; Doucet et al., 1999). We found that the somata of ventrotubercular cells that had low percent apposition (<50%) were significantly smaller than those having high percent apposition (>50%). In addition, planar cells were the dominant cell type within the isofrequency band, whereas radiate cells were more numerous outside the band. Likewise, in the isofrequency band, cells with low percent apposition outnumbered cells with high percent apposition by approximately 2 to 1. This trend was exactly reversed outside the isofrequency band. In Figure 9, we summarize the distribution of all the neurons with respect to the isofrequency band. Notice that the distributions for cells having low and high percent appositions match those predicted for planar and radiate cells, respectively (Fig. 2). These observations were consistent with the idea that radiate cells tend to receive many synapses on the soma, whereas planar cells tend to receive few.

The distribution of cells having low percent apposition needs to be addressed further. With LM, we previously reported that the projection of planar cells to the DCN was organized tonotopically (Doucet and Ryugo, 1997). However, EM showed that four of 17 neurons that had low percent apposition (supposedly planar cells) were dorsal to the band (Fig. 9). These four cells were labeled with injections in DCN regions tuned to lower frequencies. Several possible explanations emerge: (1) some radiate cells have low percent appositions; (2) a few planar cells have nontopographic projections to the DCN; or (3) these four neurons are planar cells labeled via an "axons of passage" artifact. We propose that this last possibility is the most likely explanation. This proposition is supported by the lack of cells with low percent apposition values lying ventral to the isofrequency band, presumably because axons of planar cells in this region do not pass near the injection site (see the gray planar cell in the low frequency region of the VCN in Fig. 2).

Using EM, we described what appears to be a third type of ventrotubercular cell, the adendritic neuron. Resembling neurons with high percent apposition, the somata of adendritic cells were covered with synaptic endings (86.5 ± 2.9%). The cell bodies of adendritic neurons, however, were half the size of those having high percent apposition. Further, we found no LM or EM evidence that they had dendrites. Rather, adendritic cells had thin appendages that extended into the neuropil between the synaptic endings (Fig. 8). The adendritic cells would have been considered part of sectioned neurons or perhaps

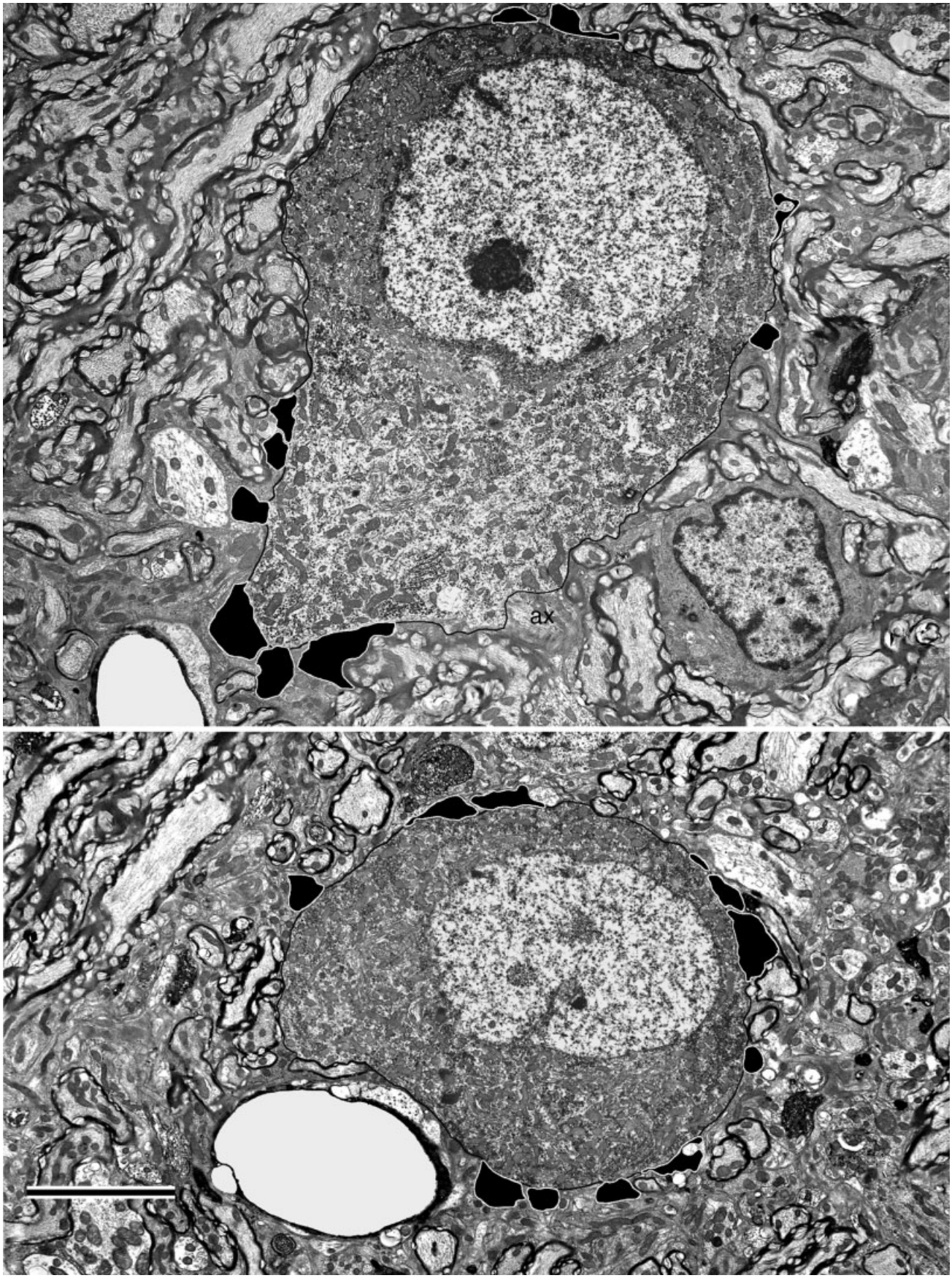

Fig. 5. Electron micrographs of typical ventral cochlear nucleus planar neurons that were labeled and found within the isofrequency band. The soma of each cell is outlined in black. Axosomatic endings are outlined in white and filled in black. Most planar cells had an eccentrically placed nucleus, in contrast to radiate cells with a more centrally located nucleus. Top: This cell (24-2, rat 3-5-01) demonstrates relatively few axosomatic endings (31.5% of surface) consistent with type I stellate cells of cats (Cant, 1981). Endings tend to cluster near the dendrosomatic junction on the lower left. The axon is labeled (ax) where it emerges from the cell body. Bottom: Another labeled cell (24-5, rat 3-05-01) in the isofrequency band with low percent apposition (44.2%). Scale bar = 5 μm for both micrographs.

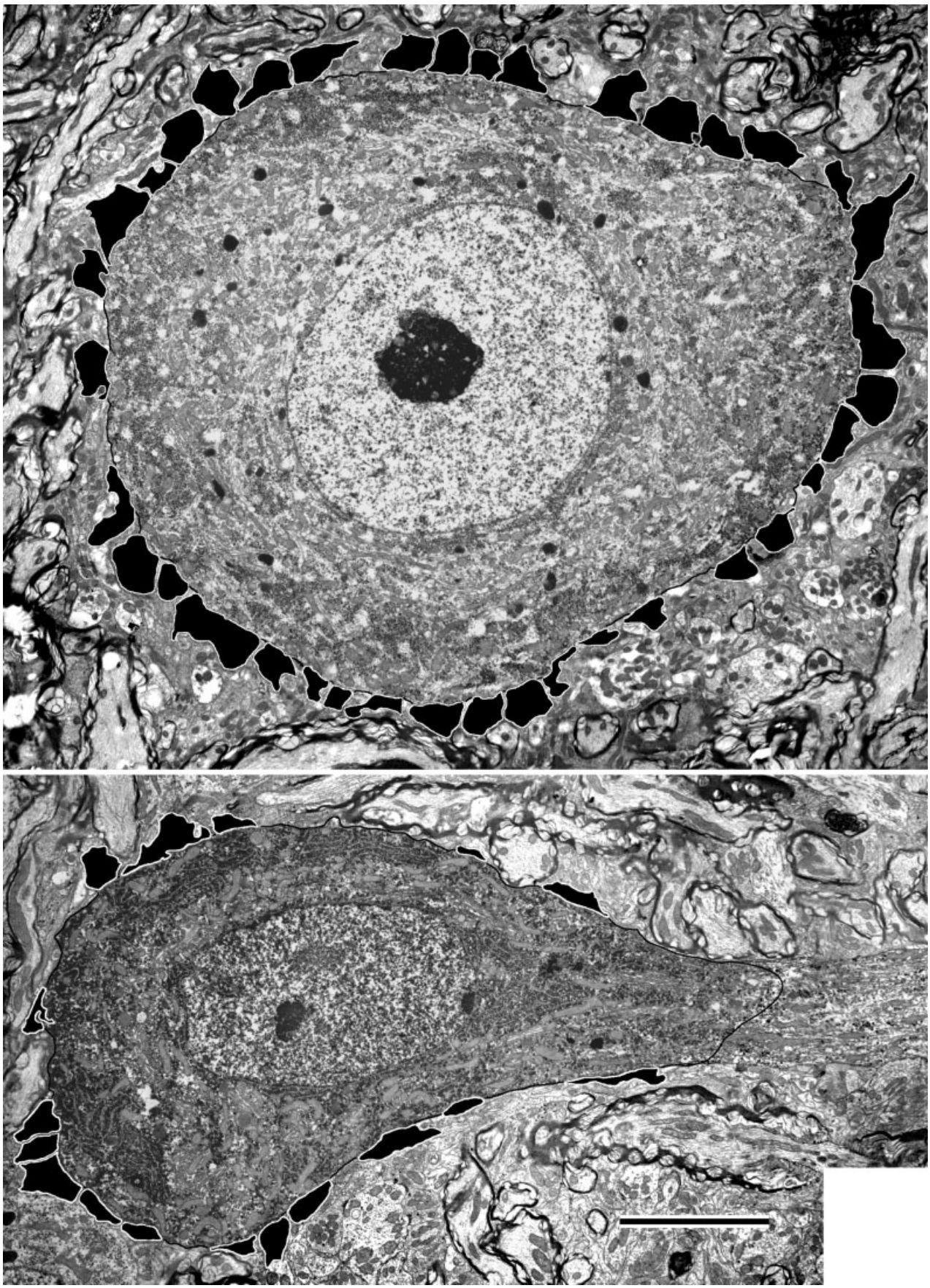

Fig. 6. Electron micrographs of labeled radiate cells outside the isofrequency band, demonstrating their centrally placed nuclei. Top: Giant radiate cell demonstrates features of type II stellate cells (30-5, rat 3-05-01). Numerous terminal endings stud the somatic surface (78.4%). Bottom: Radiate cell (20-2, rat 2-26-01) with features occasionally noted in neurons outside the isofrequency band. These features include stacks of endoplasmic reticulum, especially around the nucleus. This cell also demonstrates a high percent apposition (72.1% of surface). Scale bar = 5 μm for both micrographs.

incompletely-filled planar cells because of their small somata.

On the basis of LM observations, we proposed that the tonotopic projection from the VCN to the DCN consisted almost entirely of planar cells (Doucet and Ryugo, 1997). EM examination showed that, within the isofrequency band, most neurons (54%) had low percent appositions (probably planar cells). High percent apposition cells comprised 25% (probably radiate cells), and adendritic neurons represented 21% of this population. Thus planar cells with low percent appositions still appear to dominate the "on-frequency" projection to the DCN.

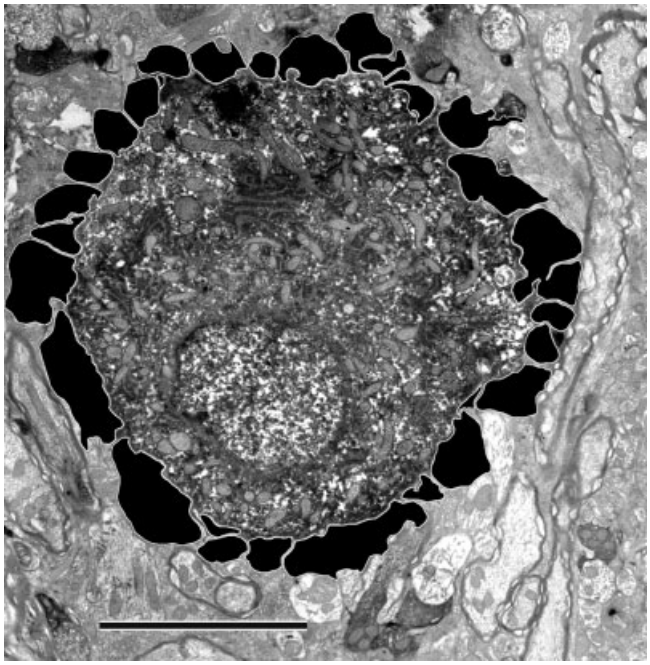

Fig. 7. Electron micrograph of a small labeled cell (23-2, rat 2-26-01) within the isofrequency band that had a very high percent apposition (90.1%). These cells are referred to as adendritic neurons and were found exclusively within the isofrequency band. Scale bar = 5 μm.

Type I and II multipolar/stellate cells: Interspecies comparisons

A random sample of stellate cells in the cat described two distinct classes of neurons based on their ultrastructure (Cant, 1981). Most cells had percent appositions less than 35% (type I), and some had percent appositions greater than 70% (type II). Few cells had percent appositions between these two values. In a different study, intracellular recordings were made from VCN multipolar cells in cats, their responses to sound were characterized, and the neurons subsequently were filled with horseradish peroxidase (Smith and Rhode, 1989). Five units from the physiologic class of ChS were type I stellate cells. In contrast, four OnC units were type II stellate cells. Both classes projected a collateral axon into the DCN. From the results of these two studies, one could predict that an extracellular injection of BDA into the DCN would fill a collection of type I and type II cells. In the present study, however, we found that 45% of our sample of ventrotubercular cells in the rat had percent appositions between 35% and 70%, values outside the classic definition of type I and type II cells.

There are at least two reasons for the less pronounced dimorphism in synaptic profiles observed in the rat. First, some evidence in the literature suggested that the synaptic profiles of rat multipolar cells differ from those in other

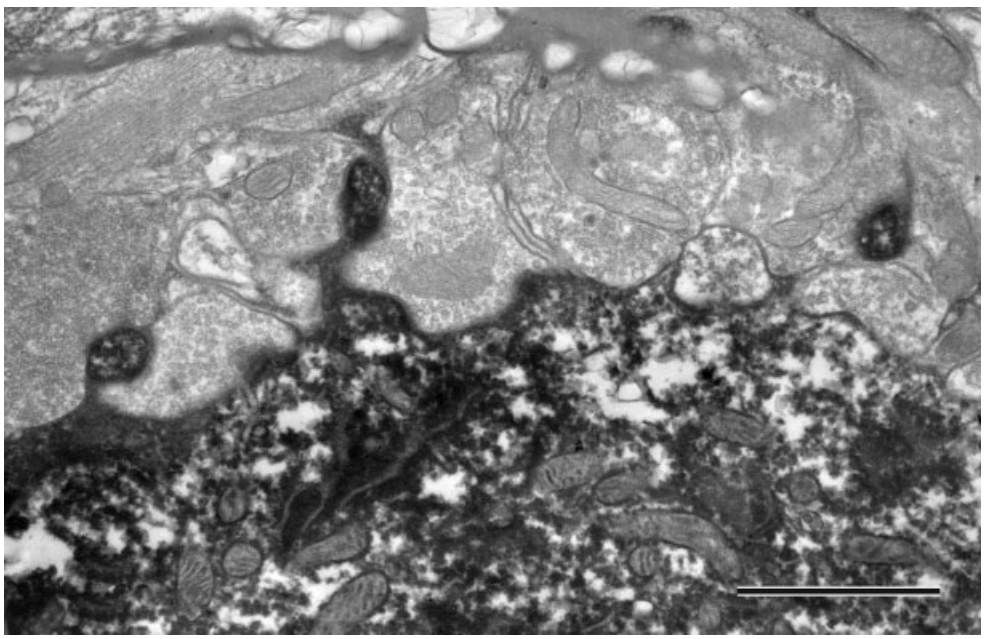

Fig. 8. Electron micrograph of the surface of an adendritic cell, illustrating the numerous somatic projections into the surrounding neuropil. These cytoplasmic filopodia often contained dense material and interdigitated with contacting terminals. Scale bar = 1 μm.

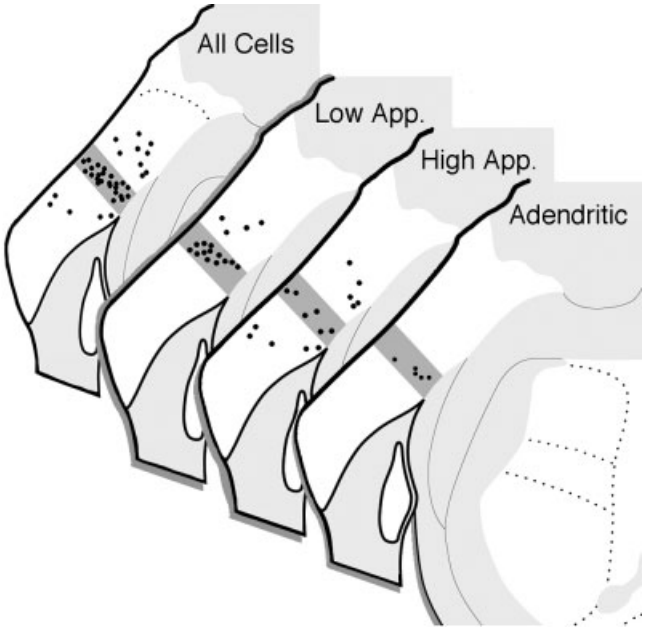

Fig. 9. Distribution of ventrotubercular cells relative to the isofrequency band after an extracellar injection of biotinylated dextran amine into a limited frequency region of the dorsal cochlear nucleus. The dark-shaded stripe in the ventral cochlear nucleus (VCN) represents the isofrequency band produced in each case. The labeled cells were distributed in the posterior VCN and the auditory nerve root, but, for this figure, they are displayed within one coronal section. The locations of all examined ventrotubercular cells are plotted in the far left outline of the cochlear nucleus. These neurons were partitioned into three classes according to ultrastructural criteria: cells with low percent apposition (Low App., apposition <50%), cells with high percent apposition (High App., apposition >50%), and adendritic cells. The distribution of low and high percent apposition cells matches that predicted for planar and radiate cells, illustrated in Figure 2. The distribution of adendritic neurons suggested that higher apposition cells are more medial in the nucleus, but this observation was not statistically significant.

species. For example, the ultrastructural morphology of multipolar cells that project to the contralateral IC was examined in cat, chinchilla, and rat. In cat and chinchilla, only type I multipolar cells were labeled by injections of horseradish peroxidase into the IC, and all had percent appositions less than 40% (Cant, 1982; Josephson and Morest, 1998). For the rat, most VCN neurons that projected to the IC also had percent appositions less than 40% (72 of 89; Alibardi, 1998a). However, the remainder had percent appositions between 52% and 85%. Unlike the cat and chinchilla, rat multipolar cells that project to the IC exhibited a wider range of synaptic profiles. This observation indicated that synaptic coverage of multipolar cell somata do not distinguish different types of stellate cells in rats.

A second possibility is that the synaptic profiles for multipolar cells vary along a continuum for all species, and that the differences seen across studies are due to different sampling methods. Multipolar cells are numerous, found throughout the anterior and posterior VCNs, and are thought to be composed of several distinct subclasses. However, EM studies are labor intensive, so only a small subset of multipolar cells can be realistically examined for any study. The two reports that analyzed IC-projecting cells in the cat and chinchilla sampled cells from the anterior VCN (Cant, 1982; Josephson and Morest, 1998). A study of IC-projecting multipolar neurons in rats examined neurons in the anterior and posterior VCNs and observed cells with low and high percent apposition (Alibardi, 1998a). Sampling more multipolar neurons over a broader region of the VCN may be necessary to reveal the underlying variability in their synaptic profiles.

Different sampling methods also may account for the different synaptic profiles reported for ventrotubercular cells in cats and rats. Intracellular recording and staining of fewer than 10 chopper cells found that only type I and type II cells project to the DCN (Smith and Rhode, 1989). In contrast, labeling and examining more ventrotubercular cells with an extracellular injection of BDA into the DCN of rats showed that they have a continuum of synaptic profiles (Alibardi, 2001; present study). These differences would be consistent if one supposes that the small number of intracellularly-filled ventrotubercular neurons in cat happened to fall in the extreme ends of the underlying distribution of percent apposition.

Functional considerations

The distribution of synaptic profiles among stellate cells is important in understanding the link between structure and function for these neurons. Stellate cells correspond to the physiologic classes referred to as *chopper* and *onset units* of single-unit studies (Rhode et al., 1983; Rouiller and Ryugo, 1984). Investigators who extracellularly recorded from VCN neurons found a variety of chopper and onset neurons such as ChS, OnC, transient choppers, On-L neurons, etc. (Pfeiffer, 1966; Bourk, 1976; Blackburn and Sachs, 1989; Winter and Palmer 1990; Rhode and Greenberg, 1992). There are also a significant number of physiologic units referred to as "unusual" that do not fit into any of these categories (e.g., Blackburn and Sachs, 1989). These classes are postulated to represent distinct functional subtypes that play different roles in sound processing. But could they actually exhibit the same amount of "gradation" in their physiologic properties as the stellate cells show in their morphology? What are the neural mechanisms that underlie this physiologic variability? Differences with respect to intrinsic mechanisms such as the types or distribution of channels could contribute to this variety, and some clear distinctions between stellate cells have been observed (Oertel et al., 1988; Manis and Marx, 1991; Oertel, 1991; Ferragamo et al., 1998). Modeling studies suggested that the number and types of synapses on the cell body play an important role in determining the responses to sound of multipolar cells (Banks and Sachs, 1991; Hewitt and Meddis, 1993; Wang and Sachs, 1995). We found that the percent appositions of ventrotubercular cells, a subset of VCN multipolar cells, vary along a continuum from low to high. More work is needed to determine the types and sources of endings on stellate cells and on the details of their intrinsic mechanisms. These data will help us better understand how structural variability might generate the wide variety of chopper and onset subclasses found in the cochlear nucleus.

ACKNOWLEDGMENTS

We thank the anonymous reviewers for their helpful criticisms. We gratefully acknowledge the technical assistance of Kate Chefer, Jenna Los, and Alison Wright.

LITERATURE CITED

Adams JC. 1979. Ascending projections to the inferior colliculus. J Comp Neurol 183:519–538.

Adams JC. 1983. Multipolar cells in the ventral cochlear nucleus project to the dorsal cochlear nucleus and the inferior colliculus. Neurosci Lett 37:205–208.

Alibardi L. 1998a. Ultrastructural and immunocytochemical characterization of neurons in the rat ventral cochlear nucleus projecting to the inferior colliculus. Ann Anat 180:415–426.

Alibardi L. 1998b. Ultrastructural and immunocytochemical characterization of commissural neurons in the ventral cochlear nucleus of the rat. Ann Anat 180:427–438.

Alibardi L. 2001. Fine structure and neurotransmitter cytochemistry of neurons in the rat ventral cochlear nucleus projecting to the ipsilateral dorsal cochlear nucleus. Ann Anat 183:459–469.

Banks MI, Sachs MB. 1991. Regularity analysis in a compartmental model of chopper units in the anteroventral cochlear nucleus. J Neurophysiol 65:606–609.

Blackburn CC, Sachs MB. 1989. Classification of unit types in the anteroventral cochlear nucleus: post-stimulus time histograms and regularity analysis. J Neurophysiol 62:1303–1329.

Blackburn CC, Sachs MB. 1992. Effects of off-BF tones on responses of chopper units in ventral cochlear nucleus. I. Regularity and temporal adaptation patterns. J. Neurophysiol 68:124–143.

Bourk TR. 1976. Electrical responses of neural units in the anteroventral cochlear nucleus of the cat [doctoral dissertation]. Cambridge: Massachusetts Institute of Technology.

Bourk TR, Mielcarz JP, Norris BE. 1981. Tonotopic organization of the anteroventral cochlear nucleus of the cat. Hear Res 4:215–241.

Brawer JR, Morest DK, Kane EC. 1974. The neuronal architecture of the cochlear nucleus of the cat. J Comp Neurol 155:251–300.

Cant NB. 1981. The fine structure of two types of stellate cells in the anterior division of the anteroventral cochlear nucleus of the cat. Neuroscience 6:2643–2655.

Cant NB. 1982. Identification of cell types in the anteroventral cochlear nucleus that project to the inferior colliculus. Neurosci Lett 32:241–246.

Doucet JR, Ryugo DK. 1997. Projections from the ventral cochlear nucleus to the dorsal cochlear nucleus in rats. J Comp Neurol 385:245–264.

Doucet JR, Ross AT, Gillespie MB, Ryugo DK. 1999. Glycine immunoreactivity of multipolar neurons in the ventral cochlear nucleus which project to the dorsal cochlear nucleus. J Comp Neurol 408:515–531.

Evans EF, Nelson PG. 1973. The responses of single neurones in the cochlear nucleus of the cat as a function of their location and anesthetic state. Exp Brain Res 17:402–427.

Ferragamo MJ, Golding NL, Oertel D. 1998. Synaptic inputs to stellate cells in the ventral cochlear nucleus. J Neurophysiol 79:51–63.

Hackney CM, Osen KK, Kolston J. 1990. Anatomy of the cochlear nuclear complex of guinea pig. Anat Embryol 182:123–149.

Hewitt MJ, Meddis R. 1993. Regularity of cochlear nucleus stellate cells: a computational modeling study. J Acoust Soc Am 93:3390–3399.

Josephson EM, Morest DK. 1998. A quantitative profile of the synapses on the stellate cell body and axon in the cochlear nucleus of the chinchilla. J Neurocytol 27:841–864.

Lorente de Nó R. 1981. The primary acoustic nuclei. New York: Raven Press.

Manis PB, Marx SO. 1991. Outward currents in isolated ventral cochlear nucleus neurons. J Neurosci 11:2865–2880.

Oertel D. 1991. The role of intrinsic neuronal properties in the encoding of auditory information in the cochlear nuclei. Curr Opin Neurobiol 1:221–228.

Oertel D, Wu SH, Hirsch JA. 1988. Electrical characteristics of cells and neuronal circuitry in the cochlear nuclei studied with intracellular recordings from brain slices. In: Edelman GM, Gall WE, Cowan WM, editors. Auditory function: neurobiological basis of hearing. New York: John Wiley & Sons. p 313–336.

Oertel D, Wu SH, Garb MW, Dizack C. 1990. Morphology and physiology of cells in slice preparations of the posteroventral cochlear nucleus of mice. J Comp Neurol 295:136–154.

Oliver DL. 1987. Projections to the inferior colliculus from the anteroventral cochlear nucleus in the cat: possible substrates for binaural interaction. J Comp Neurol 264:24–46.

Osen KK. 1969. Cytoarchitecture of the cochlear nuclei in the cat. J Comp Neurol 136:453–482.

Ostapoff EM, Morest DK, Parham K. 1999. Spatial organization of the reciprocal connections between the cat dorsal and anteroventral cochlear nuclei. Hear Res 130:75–93.

Palmer AR, Jiang D, Marshall DH. 1996. Responses of ventral cochlear nucleus onset and chopper units as a function of signal bandwidth. J Neurophysiol 75:780–794.

Pfeiffer RR. 1966. Classification of response patterns of spike discharges for units in the cochlear nucleus: tone burst stimulation. Exp Brain Res 1:220–235.

Rhode WS, Greenberg S. 1992. Physiology of the cochlear nuclei. In: Popper AN, Fay RR, editors. The mammalian auditory pathway: neurophysiology. New York: Springer-Verlag. p 94–152.

Rhode WS, Oertel D, Smith PH. 1983. Physiological response properties of cells labeled intracellularly with horseradish peroxidase in cat ventral cochlear nucleus. J Comp Neurol 213:448–463.

Rose JE, Galambos R, Hughes JR. 1959. Microelectrode studies of the cochlear nuclei of the cat. Bull Johns Hopkins Hospital 104:211–251.

Rouiller EM, Ryugo DK. 1984. Intracellular marking of physiologically characterized cells in the ventral cochlear nucleus of the cat. J Comp Neurol 225:167–186.

Ryugo DK, May SK. 1993. The projections of intracellularly labeled auditory nerve fibers to the dorsal cochlear nucleus of cats. J Comp Neurol 329:20–35.

Ryugo DK, Willard FH. 1985. The dorsal cochlear nucleus of the mouse: a light microscopic analysis of neurons that project to the inferior colliculus. J Comp Neurol 242:381–396.

Schofield BR, Cant NB. 1996. Origins and targets of commissural connections between the cochlear nuclei in guinea pigs. J Comp Neurol 375: 128–146.

Smith PH, Rhode WS. 1989. Structural and functional properties distinguish two types of multipolar cells in the ventral cochlear nucleus. J Comp Neurol 282:595–616.

Snyder RL, Leake PA. 1988. Intrinsic connections within and between cochlear nucleus subdivisions in cat. J Comp Neurol 278:209–225.

Spirou GA, May BJ, Wright DD, Ryugo DK. 1993. Frequency organization of the dorsal cochlear nucleus in cats. J Comp Neurol 329:36–52.

Wang X, Sachs MB. 1995. Transformation of temporal discharge patterns in a ventral cochlear nucleus stellate cell model: Implications for physiological mechanisms. J Neurophysiol 73:1600–1616,

Warr WB. 1982. Parallel ascending pathways from the cochlear nucleus: neuroanatomical evidence of functional specialization. In: Neff WD, editor. Contributions to sensory physiology. New York: Academic Press. p 1–38.

Weedman DL, Pongstaporn T, Ryugo DK. 1996. Ultrastructural study of the granule cell domain of the cochlear nucleus in rats: mossy fiber endings and their targets. J Comp Neurol 369:345–360.

Wenthold RJ. 1987. Evidence for a glycinergic pathway connecting the two cochlear nuclei: an immunocytochemical and retrograde transport study. Brain Res 415:183–187.

Winter IM, Palmer AR. 1990. Responses of single units in the anteroventral cochlear nucleus of the guinea pig. Hear Res 44:161–178.

Young ED, Brownell WE. 1976. Responses to tones and noise of single cells in dorsal cochlear nucleus of unanesthetized cats. J Neurophysiol 39: 282–300.

Young ED, Robert J-M, Shofner WP. 1988. Regularity and latency of units in ventral cochlear nucleus: implications for unit classification and generation of response properties. J Neurophysiol 60:1–29.